Probing Delocalization in Stable Silylenes: Core Excitation Spectra of Si(NRCH=CHNR), Si(NRCH$_2$CH$_2$NR), H$_2$Si(NRCH=CHNR), and H$_2$Si(NRCH$_2$CH$_2$NR) (R = ^{t}Bu)

Stephen G. Urquhart,[†,‡] Adam P. Hitchcock,*[,†] John F. Lehmann,[†] and Michael Denk[§]

Department of Chemistry, McMaster University, Hamilton, Ontario, Canada L8S 4M1, and Department of Chemistry, University of Toronto, Mississauga, Ontario, Canada L5L 1C6

Received October 21, 1997

The silicon 1s, 2p, and 2s, carbon 1s, and nitrogen 1s gas-phase core excitation spectra are reported for two stable divalent silylenes, Si(NRCH=CHNR) and Si(NRCH$_2$CH$_2$NR) (R = ^{t}Bu), and for the two analogous tetravalent dihydridosilane molecules, H$_2$Si(NRCH=CHNR) and H$_2$Si(NRCH$_2$CH$_2$NR) (R = ^{t}Bu). The nature of the excited states arising from one-electron core → π^* and core → σ^* excitations at different sites on the silylene ring are examined by relating the changes in the spectra of these compounds to differences in their molecular structure. The variations in the intensities of core → π^* transitions in these spectra probe the extent of delocalization in the π-electron manifold and, thus, allow us to investigate the nature of π stabilization in heterocycles containing divalent silicon. Low-lying transitions to a π^*(Si−N) level observed in all core edge spectra strongly support the existence of π-delocalization in the C=C unsaturated silylene. Ab initio calculations are used to confirm spectral assignments.

1. Introduction

The two silylene compounds Si(NRCH=CHNR) (**1**, *unsaturated silylene*) and Si(NRCH$_2$CH$_2$NR) (**2**, *saturated silylene*) (R = ^{t}Bu, see Scheme 1) are remarkable examples of molecules containing a stable divalent and dicoordinate silicon.[1] In particular, the exceptional stability of the unsaturated silylene (**1**) has been attributed to cyclic $(4n + 2)$ π delocalization.[2] The high stability of these compounds and especially their volatility allows for an experimental investigation of divalent Si at a fairly sophisticated level. The electronic structures of unsaturated silylene (**1**), saturated silylene (**2**), and the dihydridosilane analogues H$_2$Si(NRCH=CHNR) (**3**) and H$_2$Si(NRCH$_2$CH$_2$NR) (**4**) have been examined previously by He(I) and He(II) photoelectron spectroscopy (PES) and ab initio MO calculations.[2] For **1**, this PES study demonstrated that the Si 3p orbital contributes to and stabilizes the π HOMO through significant Si−N π bonding. However, comparison of the PES spectrum of the C=C unsaturated silylene (**1**) with that of the C−C saturated silylene (**2**) and the unsaturated dihydridosilane analogue (**3**) demonstrated that the energy of the lone pair on Si was not greatly affected by the saturation of carbon and that the π HOMO ($2b_2$) of **1** is stabilized by the C=C π bond.[2]

Scheme 1

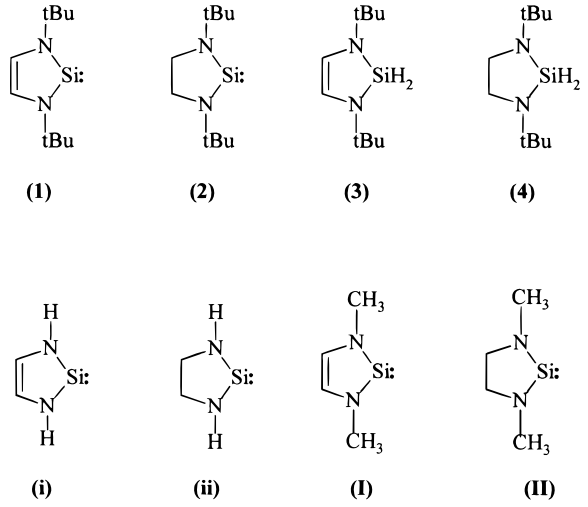

These silylene compounds are period 3 analogues of carbenes. After early studies by Wanzlick,[3] the chemistry of stable carbenes[3−10] was reopened by Arduengo and co-workers in 1991 with the structural character-

* To whom correspondence should be addressed. Email: aph@mcmaster.ca.
[†] McMaster University.
[‡] Present address: Department of Physics, North Carolina State University, Raleigh, NC 27696-7518.
[§] University of Toronto.

(1) Denk, M.; Hayashi, R. K.; West, R. *J. Chem. Soc., Chem. Commun.* **1994**, 33. Denk, M.; Lennon, R.; Hayashi, R.; West, R.; Belakov, A. V.; Verne, H. P.; Haaland, A.; Wagner, M.; Metzler, N. *J. Am. Chem. Soc.* **1994**, *116*, 2691.

(2) Denk, M.; Green, J. C.; Metzler, N.; Wagner, M. *J. Chem. Soc., Dalton Trans.* **1994**, 1004, 2405. Arduengo, A. J.; Bock, H.; Chen, H.; Denk, M.; Dixon, D. A.; Green, J. C.; Hermann, W. A.; Jones, N. L.; Wagner, M.; West, R. *J. Am. Chem. Soc.* **1994**, *116*, 6641.

(3) Wanzlick, H.-W.; Schikora, E. *Chem. Ber.* **1961**, *94*, 2389. Wanzlick, H.-W.; Lachmann, B.; Schikora, E. *Ibid.* **1965**, *98*, 3170. Wanzlick, H.-W.; Schönherr, H. J. *Angew. Chem.* **1968**, *80*, 153. Wanzlick, H.-W.; Schönherr, H. J. *Angew. Chem., Int. Ed. Engl.* **1968**, *7*, 142. Regitz, M. *Methoden Org. Chem. (Houben-Weyl) 4th ed.* **1989**, *E19b* (parts 1 and 2).

S0276-7333(97)00918-7 CCC: $15.00
Publication on Web 05/05/1998

ization of carbene counterparts to species **1** but with 1-adamantyl at the N atom.[4] Stable carbenes are now easily accessible and show a rich reaction chemistry.[4−7] The divalent germylene analogues have also been synthesized and have been shown to generate germanium films upon thermal decomposition.[11] Computational studies[9] have confirmed that these compounds possess aromatic stabilization, as concluded for the silylenes.[2] The preparation of a stable saturated carbene by Arduengo et al.[9] and isolation of the stable bis(diisopropylamino)carbene by Alder et al.[10] demonstrates that neither aromatic stabilization nor the constraints resulting from ring geometry are necessary to obtain stable diaminocarbenes. Further investigation of the electronic structure of carbenes and silylenes is of interest to better understand the critical factors in their remarkable stability.

Core excitation spectroscopy,[12−14] also known as NEXAFS (near edge X-ray absorption fine structure) or XANES (X-ray absorption near edge spectroscopy) with X-ray excitation or ISEELS (inner shell electron energy loss spectroscopy) with electron impact excitation, is complementary to PES for studies of the electronic structure of molecules. While PES probes the energy and character of *bound* electronic levels, core excitation spectroscopy probes the *unoccupied* electronic structure. In addition, unlike PES, core excitation spectroscopy is a *site*- and *symmetry*-sensitive probe of the electronic structure. The core excitation spectrum is the sum of the contributions from each atomic site in the molecule. Site sensitivity arises because the spectrum of each atomic site is sensitive to both the charge on the atom (core level shift) and the influence of the chemical environment on the unoccupied electronic structure at the site. Symmetry sensitivity arises from the atomic propensity model for electric dipole core excitation transitions. In this model, the intensity of a feature identified as a one-electron core excitation to a particular molecular orbital (MO) can be related to the contribution of atomic orbitals of appropriate symmetry to that MO. For example, Si 1s spectra of the silylenes **1** and **2** are dominated by local Si 1s → Si 3p excitation; therefore, these spectra sample the Si 3p density of the unoccupied MOs. Comparison of electric-dipole core excitation from core edges of different symmetry and from different atomic sites allows mapping of the spatial distribution and symmetry of the unoccupied electronic levels. The silylene molecules investigated here are exceptional examples in this regard. Each inequivalent site in the heterocycle ring of **1** and **4** is occupied by a different element, and therefore, each corresponding atomic core edge represents a discrete electronic environment.

With the exception of the Si 1s spectrum of SiO[15] and the Si 2p spectrum of plasma-generated Si^{2+},[16] gas-phase core excitation spectroscopy has only been applied to stable tetravalent silicon compounds.[14] Six-coordinate silicon has been investigated in the solid phase: Si 1s and Si 2p spectra of α-quartz, stishovite,[17] and silicon diphosphate[18] clearly demonstrate that core excitation spectra are quite sensitive to a change in the coordination number of silicon from four to six. Since the silylene unit contains dicoordinate divalent silicon,[1] similar dramatic effects are expected.

This paper presents the silicon (1s, 2s, 2p), carbon (1s), and nitrogen (1s), core excitation spectra of the silylenes **1** and **2** and the dihydridosilanes **3** and **4** (see Scheme 1). These spectra serve to identify core excited states that are specific to the silylene unit as well as the general character of the excited states arising from promotion of core electrons to the unoccupied π^* and σ^* levels of these molecules. The character of the core excited states is determined by comparing spectra from different core edges and by comparisons of the core edge spectra of molecules with different structures, empirically illustrating the spectral contribution of the differing structural components. Improved virtual orbital (IVO) ab initio calculations were employed to support our spectral assignments of **1** and **2**. Ab initio calculations have been performed on model compounds **I** and **II** which differ from **1** and **2** in that the ^{t}Bu group is replaced by a methyl group (see Scheme 1.) These calculations provide predictions of the core excitation spectra, give insight into the energy ordering and spatial character of the unoccupied molecular orbitals of the ground states of **1** and **4**, and also examine modifications of the molecular orbitals by electronic relaxation caused by the core hole.

2. Experimental Section

2.1. Compounds. The amides **1**,[1,2] **2**, **3**, and **4**[2] were synthesized according to literature methods. The silylenes **1** and **2** are solids, which were purified by sublimation. The dihydridosilanes **3** and **4** are liquids, which were purified by vacuum distillation. All compounds were handled under argon (99.999%).

2.2. Synchrotron Radiation Total Ion Yield Spectroscopy. The Si 1s gas-phase spectra of the silylenes **1** and **2** and the dihydridosilanes **3** and **4** were recorded using the Canadian Synchrotron Radiation Facility (CSRF) double-crystal monochromator at the

(4) Arduengo, A. J.; Harlow, R. L.; Kline, M. *J. Am. Chem. Soc.* **1991**, *113*, 361. Arduengo, A. J.; Rasika-Dias, H. V.; Harlow, R. L.; Kline, M. *J. Am. Chem. Soc.* **1992**, *114*, 5530.
(5) Arduengo, A. J.; Rasika-Dias, H. V.; Dixon, D. A.; Harlow, R. L.; Klooster, W. T.; Koetzle, T. F. *J. Am. Chem. Soc.* **1994**, *116*, 6812.
(6) Herrmann, W. A.; Goossen, L. J.; Köcher, C.; Artus, G. J. *Angew. Chem.* **1996**, *108*, 2980; *Angew. Chem., Int. Ed. Engl.* **1996**, *35*, 2805.
(7) Regitz, M. *Angew. Chem.* **1991**, *103*, 691; *Angew. Chem., Int. Ed. Engl.* **1991**, *30*, 674. Regitz, M. *Angew. Chem.* **1996**, *108*, 791; *Angew. Chem., Int. Ed. Engl.* **1996**, *35*, 725.
(8) Boehme, C.; Frenking, G. *J. Am. Chem. Soc.* **1996**, *118*, 2039. Heinemann, C.; Müller, T.; Apeloig, Y.; Schwartz, H. *J. Am. Chem. Soc.* **1996**, *118*, 2023.
(9) Arduengo, A. J.; Goerlich, J. R.; Marshall, W. J. *J. Am. Chem. Soc.* **1995**, *117*, 1102.
(10) Alder, R. W.; Allen, P. R.; Murray, M.; Orpen, A. G. *Angew. Chem.* **1996**, *108*, 1211; *Angew. Chem., Int. Ed. Engl.* **1996**, *35*, 1121.
(11) Hermann, W. A.; Denk, M.; Behm, J.; Scherer, W.; Klingan, F. R.; Bock, H.; Solouki, B.; Wagner, M. *Angew. Chem., Int. Ed. Engl.* **1992**, 11, 1485.
(12) Hitchcock, A. P. *Phys. Scr.* **1990**, *T31*, 159.
(13) Stöhr, J. *NEXAFS Spectroscopy*; Springer Series in Surface Science; Springer-Verlag: Berlin, 1992; Vol. 25.
(14) Hitchcock, A. P.; Mancini, D. C. *J. Electron Spectrosc.* **1994**, *67*, 1.
(15) Flank, A. M.; Karnatak, R. C.; Blancard, C.; Esteva, J. M.; Lagarde, P.; Connerade, J. P. *Z. Phys. D* **1991**, *21*, 357. Bouisset, E.; Esteva, J. M.; Karnatak, R. C.; Connerade, J. P.; Flank, M. A.; Lagarde, P. *J. Phys. B: At. Mol. Opt. Phys.* **1991**, *24*, 1609.
(16) Sayyad, M. H.; Kennedy, E. T.; Kiernan, L.; Mosnier J.-P.; Costello, J. P. *J. Phys. B: At. Mol. Opt. Phys.* **1995**, *28*, 1715.
(17) Li, D.; Bancroft, G. M.; Kasrai, M.; Fleet, M. E.; Feng, X. H.; Tan, K. H.; Yang, B. X. *Solid State Commun.* **1993**, *87*, 613.
(18) Li, D.; Bancroft, G. M.; Kasrai, M.; Fleet, M. E.; Feng, X. H.; Tan, K. H. *Am. Mineral.* **1994**, *79*, 785.

Aladdin Synchrotron of the University of Wisconsin at Madison.[19] The monochromator energy scale was calibrated by setting the inflection point of the Si 1s spectrum of crystalline Si to 1839.2 eV.[20] The gas-phase spectra were recorded at 0.8 eV energy resolution using total ionization yield detection. The signal from the ~10 cm long chamber was recorded simultaneously with that of the incident photon flux, I_o (monitored using a N_2-filled ionization chamber separated from the sample by a Be window) and the sample pressure (measured with a capacitance manometer). After normalization to correct for I_o and pressure variations, the total ion yield spectra were converted to an absolute oscillator strength scale by setting the Si 1s intensity to the atomic value of 0.16×10^{-2} eV^{-1} at 1860 eV.[21,22]

2.3. Electron Energy-Loss Spectroscopy. The inner-shell electron energy-loss spectrometer and operating procedures have been described previously.[12] The spectra were obtained using inelastic scattering conditions where dipole transitions dominate (2.5 keV final electron energy, 2° scattering angle) with an energy resolution of 0.7 eV full-width at half-maximum (fwhm). Heating the solid samples (**1** and **2**) to ~60 °C was sufficient to generate adequate vapor pressure in the gas cell. The vapor of the dihydridosilanes **3** and **4** was introduced into the gas cell through a leak valve after degassing the liquid by several freeze−pump−thaw cycles. Absolute energy scales were established by recording the spectrum of a stable mixture of the compound and CO, N_2, or CO_2 (standard calibrant species) as documented in the tables of spectral assignments. The as-recorded ISEELS spectra were converted to relative optical spectra and normalized to tabulated atomic oscillator strengths (for C 1s and N 1s) using procedures discussed elsewhere.[14] For the Si 2p and Si 2s regions, the relative values were normalized to the absolute Si 2p oscillator strength of SiH_4 in the featureless, atomic-like 145−151 eV region.[23]

2.4. Ab Initio Calculations. To discuss the core excitation spectra of the silylenes **1** and **2** and the dihydridosilanes **3** and **4**, it is necessary to have a clear picture of the relative energies and spatial character of the final electronic states. Previously, we used extended Hückel molecular orbital (EHMO) calculations for calculating core excitation spectra.[24] However, EHMO results for the ground state of **1** (carried out with and without Si 3d orbitals; results not shown) did not correctly reproduce the energy sequence of the valence ion states (i.e., the ordering of the occupied π MOs) as observed by PES and as calculated at an ab initio (MP4/HF/6-31G*) level.[2] If EHMO is inadequate for occupied MOs, it may not be appropriate for examining unoccupied MOs of silylene molecules.

Table 1. Total Energies and Geometries of the Model Compounds i and ii[a] and I and II

model	symmetry[b]	energy (HF)[c] (au)	energy (MP2)[d] (au)
i	C_{2v}	−475.891	−476.549
ii	C_2	−477.059	−477.717
I	C_{2v}	−553.704[e]	
II	C_2	−554.838[e]	

	bond lengths (Å)			bond angles (deg)		
model	Si−N	N−C(1)	C(1)−C(1′)	N−Si−N	Si−N−C(1)	N−C(1)−C(1)
i, **I**	1.742	1.390	1.332	86	115	113
ii, **II**	1.720	1.456	1.536	83	120	118

[a] Calculations performed on geometry-optimized structures (HF-6-31G*) of **i** and **ii**, with addition of a standard methyl group at the known N−Me distance.[1] [b] Symmetries defined for molecules lying in the *xz* plane. [c] Energies from a single-point calculation at the HF-6-31G* level. [d] Energies from a single-point calculation at the MP2/6-31G* level. [e] Energy for the ground state using the basis set optimized for the Si 1s core level calculation.

For this study, we have employed ab initio calculations using Kosugi's GSCF3 package,[25−26] which is highly optimized for accurate calculations of core excitation spectra. GSCF3 is based upon the improved virtual orbital (IVO) approximation,[27] which explicitly includes the core hole in the Hartree−Fock Hamiltonian. This is extremely important for accounting for the influence of the core hole on the unoccupied electronic structure. The relaxed Hartree−Fock potential is essential for accurately reproducing the large electronic reorganization that occurs upon inner-shell hole creation. This approach has been shown to be quite accurate in predicting term values and intensities of core excitations as well as the core-level ionization potentials.[28,29]

GSCF3 calculations have been performed on model compounds **I** and **II**, which differ from **1** and **2** in that the ^{t}Bu group is replaced by a methyl group (see Scheme 1). The geometry used for the GSCF3 calculations was based on the calculated geometry-optimized structures of **i** and **ii** in which the ^{t}Bu group of **1** and **2** is replaced by a hydrogen atom. The program SPARTAN[30] was used to provide geometry-optimized structures for **i** and **ii** through ab initio calculations at the HF/6-31G* level. Harmonic vibrational frequencies calculated at the HF/6-31G* level verify that the optimized structures represent the minima in the potential-energy surface. The methyl group was appended to the geometry-optimized structures of **i** and **ii** using literature bond lengths,[1] R(C−N) = 1.49 Å, R(C−H) = 1.09 Å, assuming that the C−N−Si angle is the same as the calculated H−N−Si angle and that the methyl group is tetrahedral. Total energies and geometries are consistent with those published previously.[2,31] Selected bond lengths and bond angles of **i** and **ii** are presented in Table 1. Note that the geometry-optimized structure of **I** is of C_{2v} symmetry, as are **iii**, **III**, and **3**; the geometry-optimized structure of **ii** (and **iv**, **IV**, and **4**) is of C_2 symmetry due

(19) Yang, B. X.; Middleton, F. H.; Olsson, B.G.; Bancroft, G. M.; Chen, J. M.; Sham, T. K.; Tan K. H.; Wallace, D. J. *Nucl. Instrum. Methods Phys. Res. A* **1992**, *316*, 422.
(20) Hitchcock, A. P.; Tyliszczak, T.; Aebi, P.; Xiong, J. Z.; Sham, T. K.; Baines, K. M.; Mueller, K. A.; Feng, X. H.; Chen, J. M.; Yang, B. X.; Lu, Z. H.; Baribeau, J. M.; Jackman, T. E. *Surf. Sci.* **1993**, *291*, 349.
(21) Thomas, M. M.; Davis, J. C.; Jacobsen, C. J.; Perera, R. C. C. *Nucl. Instrum. Methods Phys. Res. A* **1990**, *291*, 107.
(22) Henke, B. L.; Lee, P.; Tanaka, T. J.; Shimabukuro R. L.; Fujikawa, B. J. *At. Data Nucl. Data Tables* **1982**, *27*, 1.
(23) Cooper, G.; Ibuki, T.; Brion, C. E. *Chem. Phys.* **1990**, *140*, 133.
(24) Urquhart, S. G.; Hitchcock, A. P.; Priester, R. D.; Rightor, E. G. *J. Polym. Sci, Part B: Polym. Phys.* **1995**, *33*, 1603.
(25) Kosugi, N. *Theor. Chim. Acta* **1987**, *72*, 149.
(26) Kosugi, N.; Kuroda, H. *Chem. Phys. Lett.* **1980**, *74*, 490.
(27) Hunt, W. J.; Goddard, W. A., III *Chem. Phys. Lett.* **1969**, *3*, 414.
(28) Kosugi, N.; Shigemasa, E.; Yagishita, A. *Chem Phys. Lett.* **1992**, *190*, 481.
(29) Kosugi, N.; Adachi, J.; Shigemasa, E.; Yagishita, A. *J. Chem. Phys.* **1992**, *97*, 8842.
(30) *Spartan version 4.0*; Wavefunction Inc.: Irvine, CA, 1994.
(31) Blakeman, P.; Gehrhus, B.; Green, J. C.; Heinicke, J.; Lappert, M. F.; Kindermann M.; Veszprémi, T. Private communication.

Table 2. Calculated Term Values, Energies, and Oscillator Strengths for the Si 1s, N 1s, and C 1s Core Excitation Spectra of Silylene Model I and Saturated Silylene Model II

I				II			
MO	T. V. (eV)	energy (eV)	osc str (10^{-2} eV^{-1})	MO	T. V. (eV)	energy (eV)	osc str (10^{-2} eV^{-1})
			Si 1s				
$\pi^*(b_2)$	3.85	1838.63	0.584	$\pi^*(b_2)$	4.40	1838.51	0.790
$\sigma^*(b_1)$	1.82	1840.66	0.443	$\sigma^*(b_1)$	1.69	1841.21	0.404
Ryd	0.37	1842.11	0.004	Ryd	0.35	1842.55	0.000
$\pi^*(a_2)$	0.36	1842.12	0.000	σ^*	−0.05	1842.95	0.023
IP		1842.48				1842.90	
			N1s				
$\pi^*(b_2)$	3.13	400.76	0.725	$\pi^*(b_2)$	2.99	400.55	0.405
$\sigma^*(b_1)$	1.35	402.55	0.056	σ^*/Ryd	0.98	402.56	0.048
σ^*/Ryd	0.41	403.48	0.012	σ^*/Ryd	0.50	403.04	0.009
$\pi^*(a_2)$	0.36	403.54	0.106	σ^*/Ryd	−0.03	403.56	0.083
IP		403.89				403.53	
			C1s				
$\pi^*(b_2)$	2.44	288.23	0.731	σ^*/Ryd	2.30	289.24	0.036
$\pi^*(a_2)$	1.71	288.96	1.556	σ^*/Ryd	1.49	290.04	0.447
Ryd	0.99	289.68	0.325	σ^*/Ryd	0.67	290.86	0.885
$\sigma^*(b_1)$	0.15	290.7	0.058				
IP		290.67				291.53	

to out-of-plane puckering of the C−C segment of the ring. For convenience, C_{2v} labels are used throughout to discuss the *experimental* core excited states of all molecules **1** and **4**.

GSCF3 calculations were performed on the silylene model **I** and on the saturated silylene model **II**. These calculations were performed using the Gaussian-type extended basis set of Huzinaga et al.[32] A basis set of (521/41) is employed for carbon and nitrogen atoms, (4321/421) for silicon atoms, and (51) for hydrogen atoms. In these calculations, the basis set of the atom with the core hole is higher quality: (3111111 3111) for carbon 1s and nitrogen 1s calculations, and (3112121 311111) for silicon 1s calculations. A polarization function is also placed on the core excited atom.

Table 2 presents the calculated term values, excitation energies, and oscillator strengths for Si 1s, N 1s, and C 1s excitation to the unoccupied molecular orbitals corresponding to the lowest energy features in these spectra. For each species, the calculated IVO term values and oscillator strengths were combined with the calculated absolute inner-shell ionization energies to generate the predicted core excitation spectrum on an absolute energy scale. To facilitate comparison with experiment, the calculated results were broadened using Gaussian line widths of 4 eV fwhm for orbitals of eigenvalues (ϵ) above +4 eV, 1.2 eV for $+0 < \epsilon < +4$, and 0.6 eV for bound states. The results of these calculations are discussed below, in comparison to experiment.

3. Results and Discussion

3.1. Si 1s Spectra. The silicon 1s total ion yield core excitation spectra of the silylenes **1** and **2** and the dihydridosilanes **3** and **4** are presented in Figure 1. The energies and proposed assignments of the spectral features are presented in Table 3. There are two, remarkably sharp, low-lying transitions in the Si 1s spectra of the silylene compounds **1** and **2**. The previous PES study of **1** and **2**[2] indicated strong Si−N π-bonding.

(32) Huzinaga, S.; Andzelm, J.; Klobokowski, M.; Radzio-Andzelm, E.; Sasaki, Y.; Tatewaki, H. *Gaussian Basis Sets for Molecular Calculations*; Elsevier: Amsterdam, 1984.

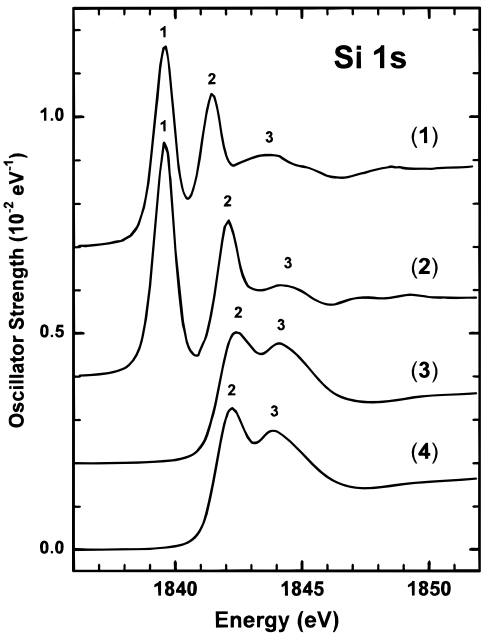

Figure 1. Si 1s oscillator strength spectra of **1**−**4** derived from background- subtracted, total ion yield X-ray absorption spectra. Offsets of 0.7, 0.4, and 0.2 (10^{-2} eV^{-1}) have been used for clarity in the spectra of **1**, **2**, and **3**, respectively.

Low-lying transitions corresponding to Si 1s excitation to the π^* lowest unoccupied molecular orbital (LUMO) were, therefore, expected in the Si 1s core spectrum. A symmetry analysis for **1** (point group, C_{2v}; molecule in *xz* plane) indicates that π^* (i.e., p_y) electronic states will be of a_2 or b_2 symmetry. However, as the Si atom is on the C_2 molecular symmetry axis of this molecule, the Si $3p_y$ orbitals cannot contribute to the a_2 symmetry π-MOs. Thus, only Si 1s → $\pi^*(b_2)$ transitions will contribute to an electric dipole excitation spectrum, although transitions to both $\pi^*(b_2)$ and $\pi^*(a_2)$ final states are possible from all other atomic sites in the molecule.

The ab initio calculations for Si 1s excited **I** predict the lowest energy feature will be associated with excitations from the Si 1s(a_1) level to the $\pi^*(b_2)$ LUMO, with a Si 1s(a_1) → $\sigma^*(b_1)$ transition at higher energy (see

Table 3. Energies (eV) and Assignments of Features in the Si 1s and 2s Spectra of Silylenes (R_2Si:) and Dihydridosilanes (R_2SiH_2)

	1		**2**		**3**		**4**		
no.	Si 1s[a]	Si 2s	Si 1s	Si 2s	Si 1s	Si 2s	Si 1s	Si 2s	assignment[b]
1	1839.56	151.9	1839.57	151.7					π^*(Si−N, b_2) $^1B_2$
2	1841.48	153.9	1842.13	154.3	1842.5	154.4	1842.25	154.2	σ^*(Si−N, b_1) $^1B_1$
3	1843.7		1844.2		1844.1	156	1843.9	156	σ^*(Si−N, a_1) $^1A_1$

[a] Calibration: Monochromator energy scale calibrated by setting the edge inflection of the Si 1s spectrum of crystalline Si to 1839.2 eV.[20] [b] C_{2v} symmetry labels are used for convenience in the case of the C_2 symmetry molecules **2** and **4**.

Table 2). Thus, the first peak in the Si 1s spectrum of **1** is assigned as the Si 1s → π^* (Si−N, b_2) transition. The second sharp peak is associated with the Si 1s → σ^*(Si−N, b_1) transition. The third weak feature in the Si 1s spectrum of **1** is assigned as Si 1s excitation to a higher energy σ^* level. Note that Si 1s → π^*(C═C, a_2) excitation is dipole forbidden.

For **2**, the Si 1s → π^*(Si−N, b_2) transition occurs at approximately the same energy as for **1** but the Si 1s → σ^*(Si−N, b_1) transition is shifted to higher energy by +0.65 eV (for convenience, C_{2v} labels are used for assigning transitions in the spectra of **2** and **4**). The calculated energy of the $\sigma^*(b_1)$ molecular orbital in **II** relative to that in **I** shifts in the same manner. Broad transitions are observed at 1843.7 and 1844.2 eV in **1** and **2**, respectively. These are attributed to Si 1s → σ^*-(Si−N) transitions.

Strong support for our Si 1s → π^* assignments in **1** and **2** is provided by the Si 1s spectra of the dihydridosilanes **3** and **4**. Consistent with the tetravalent coordination there is no signal below 1841 eV in **3** and **4**, the region where the sharp Si 1s → π^*(Si−N, b_2) transitions are observed in **1** and **2**. The Si 1s → σ^*-(Si−N, b_1) transitions around 1842 eV are broader in **3** and **4** than in **1** and **2**.

The dihydridosilanes **3** and **4** show a second strong peak at ∼1844 eV. This feature is assigned to the Si 1s → σ^*(Si−N, a_1) transition. Similar but much weaker features are seen in the Si 1s spectra of **1** and **2**. The difference in the intensity of this feature between **1** and **2** versus **3** and **4** is interesting. The atomic propensity model suggests that the A_1 state contains considerably more 3p density centered at Si in the tetrahedral dihydridosilanes **3** and **4** than in the dicoordinate silylenes **1** and **2**.

The Si 1s → σ^*(Si−N, b_1) transition in **2** is +0.65 eV higher in energy that that in **1**. The GSCF3 calculations predict the Si 1s → σ^*(Si−N, b_1) transition in **II** is +0.55 eV higher in energy than that in **I**, in good agreement. This shift consists of a +0.42 eV shift in the Si 1s binding energy and a +0.13 eV shift in the σ^*(Si−N, b_1) term value between **I** and **II** (see Table 2). The valence component (i.e., represented by the term value) of this σ^* energy shift may be related to the change in the Si−N bond length. Within the bond length correlation model, shorter/stronger bonds have associated σ^* resonances at **smaller** term values (therefore, higher energies) than longer/weaker bonds[33−35] (term value = ionization potential − transition energy). Si−N bond lengths are available from gas-phase electron diffraction for **1** and solid-state X-ray diffraction for **2**.[2] The Si−N bond is 0.034 Å *shorter* in **2** than in **1**, which should lead to a higher transition energy, as observed. This effect is very small since peak positions in core excitation spectra of *third-row* element core edges (e.g., Si, P, S) are generally less dependent on bond lengths[36] than in the core spectra of second-row elements where strong variations with bond length are observed.[33]

3.2. Si 2s Spectra. Since the core orbital symmetry is the same, the Si 2s spectra are expected to be similar to the Si 1s spectra. The background-subtracted silicon 2s electron energy-loss spectra of **1**−**4** are presented in Figure 2. The top panel of Figure 2 presents the raw Si 2p and Si 2s spectra of **1** together with the fitted power-law background-function subtracted to isolate the core edge signals. Energies and proposed assignments of the spectral features are presented in Table 3.

The Si 2s core edge is a relatively weak feature superimposed on a much larger Si 2p ionization signal. This large background makes it difficult to accurately isolate the Si 2s signal. Notwithstanding these difficulties, the Si 2s spectra are qualitatively similar to the Si 1s spectra. For **1** and **2**, the Si 2s → π^*(Si−N,b_2) and Si 2s → σ^*(Si−N, b_1) transitions are clearly resolved and the energy shift between them is similar to that observed in the Si 1s spectra. In particular, the constancy of the energy of the $\pi^*(b_2)$ and the shift in the $\sigma^*(b_1)$ features closely follows that of the corresponding Si 1s features. The two σ^* features expected in the Si 2s spectra of **3** and **4** are not clearly resolved, although it should be noted that the σ^* features in the Si 1s spectra of **3** and **4** are broader than the corresponding peaks in the Si 1s of **1** and **2**. These spectra demonstrate that Si 2s and Si 1s core excitation provide similar information. This is expected and is a useful confirmation of the atomic propensity model—core levels of the same atomic symmetry (1s, 2s) couple to the same final states with similar relative intensities.

3.3. Si 2p Spectra. The Si 2p spectra (Figure 3, Table 4) of the silylenes **1** and **2** and the dihydridosilanes **3** and **4** are quite different from the Si 1s and 2s spectra. This is consistent with the atomic propensity model, which favors excitations from p-symmetry core levels to unoccupied levels with large Si 3s or Si 3d character. Thus, Si 2p → $\pi^*(b_2)$ transitions in **1** and **2** are expected to be absent or very weak, since Si $3p_y$ atomic orbitals are expected to be the main contribution to π^* molecular orbitals. In fact, there is a weak low-energy feature at 100.9 eV in the Si 2p spectrum of both

(33) Sette, F.; Stöhr J.; Hitchcock, A. P. *J. Chem. Phys.* **1984**, *81*, 4906.
(34) Lindholm, E.; Asbrink, L.; Ljunggren, S. *J. Phys. Chem.* **1991**, *95*, 3923.
(35) Sheehy, J. A.; Gil, T. J.; Winstead, C. L.; Farren R. E.; Langhoff, P. W. *J. Chem. Phys.* **1989**, *91*, 1796.
(36) Hitchcock, A. P.; Bodeur, S.; Tronc, M. *Physica B* **1989**, *158*, 257.
(37) Bozek, J. D.; Bancroft, G. M.; Tan, K. H. *Chem. Phys.* **1990**, *145*, 131.

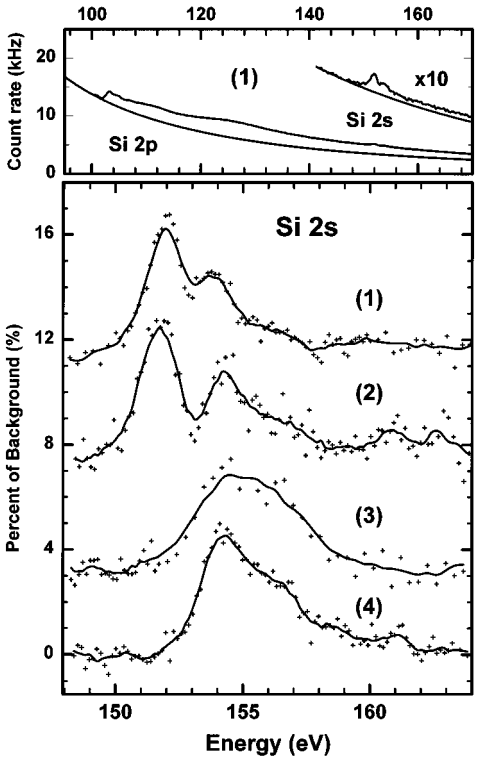

Figure 2. (top) The as-recorded inner-shell-electron energy loss spectra of **1** in the region of Si 2p and Si 2s excitation, measured using a 2.5 keV final electron energy, a 2° scattering angle, and 0.7 eV fwhm resolution. The smooth lines are fitted functions used to isolate the Si 2p and Si 2s signals by subtracting the extrapolated valence ionization and Si 2p ionization background signals. (bottom) Background-subtracted Si 2s spectra of **1**−**4**. The spectral intensity is expressed as a percent of the background signal. Offsets of 11%, 7% and 3% have been used for clarity in the spectra of **1**, **2**, and **3**, respectively. The solid line is a smoothed version of the data included as a guide to the eye.

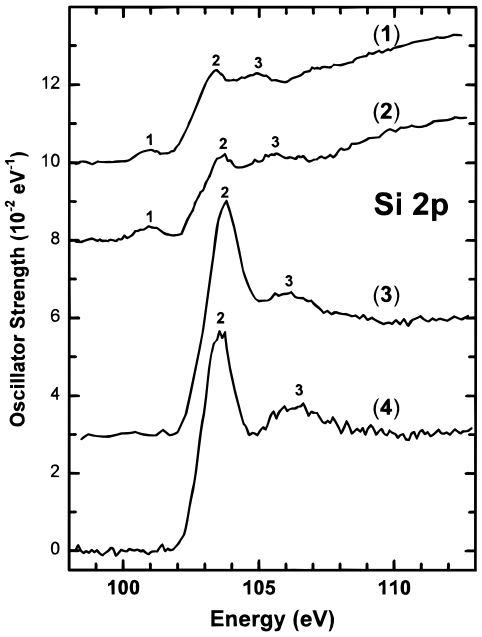

Figure 3. Si 2p oscillator strength spectra of **1**−**4** derived from background- subtracted energy-loss spectra recorded using a 2.5 keV final electron energy, a 2° scattering angle, and 0.7 eV fwhm resolution. Offsets of 10, 8, and 3 (10^{-2} eV^{-1}) have been used for clarity in the spectra of **1**, **2**, and **3**, respectively.

Table 4. Energies (eV) and Assignments of Features in the Si 2p Spectra of Silylenes (R_2Si:) and Dihydridosilanes (R_2SiH_2)

no.	1	2	3	4	assignment[e]
1	101.0	101.0			π^*(Si−N, b_2), $^1A_1$, $^1B_2$
2	103.4[a]	103.7[b]	103.8[c]	103.6[d]	σ^*(Si−N, b_1), $^1A_1$, $1B_1$
3	104.9	106.0	106.3	106.5	σ^*(Si−N, a_1), $^1A_1$, $1B_1$, $^1B_2$
4 br	112	112	113	113	ϵd
5 br	130	130	128	128	ϵd

[a] Calibration relative to the C 1s → π^* transition of CO (287.40 eV),[40] $\Delta E = -184.0$ eV. [b] Calibration relative to the N 1s → π^* transition of N_2 (401.1 eV),[40] $\Delta E = -297.4(1)$ eV. [c] Calibration relative to the C 1s → π^* transition of CO_2 (290.74 eV),[40] $\Delta E = -186.82(6)$ eV. [d] Calibration relative to the C 1s → π^* transition of CO_2,[40] $\Delta E = -187.16(5)$ eV. [e] C_{2v} symmetry labels are used for convenience in the case of the C_2 symmetry molecules **2** and **4**.

1 and **2** which we attribute to Si 2p → $\pi^*(b_2)$ transitions. Although this transition is disfavored by the atomic propensity model, in a molecular picture, Si 2p → b_2 transitions are symmetry allowed. In addition, in C_{2v} symmetry, final states of b_2 symmetry can contain a mixture of $3p_y$ and $3d_{yz}$ atomic contributions, thus permitting an "atomic propensity"-allowed Si 2p → π^*-(b_2) transition (e.g., Si 2p → Si 3d at the Si atom). The second, intense feature at 103.4 eV is attributed to a Si 2p → σ^*(Si−N, b_1) transition. At higher energy (104.9 eV) there is a broad feature that is only weakly observed in the corresponding Si *n*s spectra. This transition is assigned as a Si 2p → σ^*(Si−N, a_1) transition. There are also strong signals in the Si 2p continuum at 113 and 127 eV (see Figure 2 for **1**; not shown for **2**−**4**). These are characteristic of all Si 2p spectra and are attributed to delayed onset of the Si 2p → ϵd continuum ionization, as in previous treatments.[37]

The absence of a low-energy Si 2p → π^* transition in the spectra of the dihydridosilanes **3** and **4** supports our assignment of $\pi^*(b_2$, Si−N) to the first peak in the Si 2p spectra of **1** and **2**. Furthermore, the intensity of the near-edge features in the Si 2p spectra of **3** and **4** is much stronger than in **1** and **2**. Application of the atomic propensity model suggests that the low-energy unoccupied states in **1** and **2** are predominantly of p character—weak and formally forbidden in the Si 2p edge spectra—while the low-energy core excited states **3** and **4** have much more s and/or d character. The first and second transitions in the Si 2p spectra of **3** and **4** are assigned as Si 2p → σ^*(Si−N, b_1) and Si 2p → σ^*-(Si−N, a_1) transitions, respectively, in analogy to the Si 1s spectra.

3.4. C 1s Spectra. The C 1s oscillator strength spectra (Figure 4, Table 5) of the silylenes **1** and **2** and the dihydridosilanes **3** and **4** are the sum of contributions from three distinct carbon sites: one being the ring carbons and the other two associated with the eight carbon atoms of the *tert*-butyl ligands. For **1**−**4**, the *tert*-butyl-related features dominate the total spectrum and are essentially identical to those of isobutane[38] (see Table 5). Comparison of the two unsaturated species **1** and **3** with the two saturated species **2** and **4** reveals there is a characteristic peak around 286.5 eV which is associated with C 1s → π^*(C═C, a_2) transitions at the

(38) Hitchcock, A. P.; Ishii, I. *J. Electron Spectrosc.* **1987**, *42*, 11.

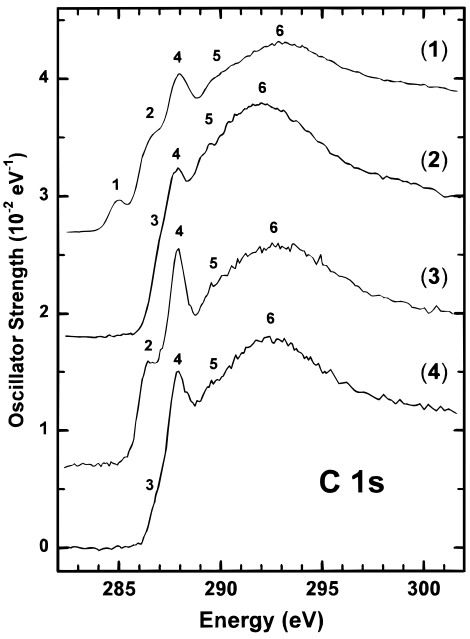

Figure 4. C 1s oscillator strength spectra of **1**−**4** derived from background- subtracted energy loss spectra. See the caption to Figure 3 for details of spectral acquisition. Offsets of 2.7, 1.8, and 0.7 (10^{-2} eV^{-1}) have been used for clarity in the spectra of **1**, **2**, and **3**, respectively.

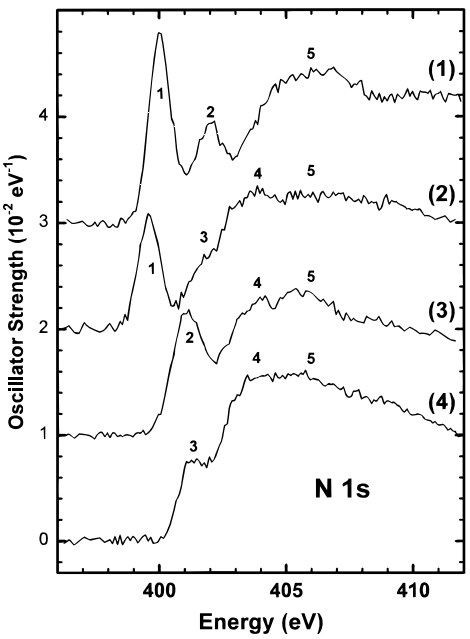

Figure 5. N 1s oscillator strength spectra of **1**−**4** derived from background- subtracted energy-loss spectra. See the caption to Figure 3 for details of spectral acquisition. Offsets of 3, 2, and 1 (10^{-2} eV^{-1}) have been used for clarity in the spectra of **1**, **2**, and **3**, respectively.

ethylene carbons in **1** and **3**. The energy and intensity of this feature does not vary substantially between the C 1s spectra of **1** and **3**. This is due to the fact that the a_2 orbital cannot mix with the Si 3p π density, on account of symmetry restrictions. The unsaturated silylene **1** has an additional peak at 285.0 eV associated with C 1s(C═C) → $\pi^*(b_2$,Si−N) transitions, which reflects the extent of delocalization of the $\pi^*(b_2)$ around the ring.

The similarity of the C 1s spectra of the two C−C saturated species **2** and **4** demonstrates that there is little interaction between the carbon atoms of the alkyl bridge and the silylene electronic density. This is in sharp contrast to the C═C unsaturated species **1** where ethylene−N−Si interactions in the $\pi^*(b_2$, Si−N) orbital generate a large difference between the spectra of **1** and **3**. In the ground state of **II**, the LUMO is the $\pi^*(b_2$, Si−N) level. A feature corresponding to C 1s → LUMO excitation is not observed in the C 1s spectrum of **2** as the $\pi^*(b_2$, Si−N) orbital does not have any density on the fully saturated carbon component of the ring.

The C 1s → σ^* region (289−295 eV) in the spectra of all four compounds is dominated by the C 1s(−CH_3) → σ^*(C−C) and C 1s(−CH_3) → σ^*(C−H) transitions associated with the *tert*-butyl groups. C 1s(t-Bu) → σ^*-(C−N) and C 1s(C═C) → σ^*(C−N) transitions are also expected to contribute in this region but are unlikely to give a well-defined structure since they are masked by the large C 1s(t-Bu) → $\sigma^*(CH_3)$/3p Rydberg intensity.

3.5. N 1s Spectra. As with the other core edge spectra, the N 1s oscillator strength spectra (Figure 5, Table 6) are strongly influenced by the molecular structure. The lowest energy N 1s feature of the silylenes **1** and **2** is assigned to N 1s → $\pi^*(b_2)$ transitions. The strong N 1s → $\pi^*(b_2)$ transition dominates the spectrum of **1**. The observation of an intense transition to this B_2 state in each of the Si, C, and N core edge spectra of **1** indicates that the $\pi^*(b_2$, Si−N) orbital is quite delocalized and, thus, there is strong mixing of ring pπ orbitals at all ring sites: Si 3p, C 2p and N 2p. In **2**, where C 2p$\pi(b_2)$ density is not present, saturation at the ring carbons weakens the N 1s → π^*-(b_2) transition intensity and shifts it to lower energy. The second feature at ∼402 eV in the N 1s spectrum of **1** and **3** is tentatively attributed to overlapping N 1s → $\sigma^*(b_1)$ and N 1s → $\pi^*(a_2)$ transitions. According to the

Table 5. Energies (eV) and Assignment of Features in the C 1s Spectra of Silylenes (R_2Si:) and Dihydridosilanes (R_2SiH_2)

no.	**1**	**2**	**3**	4	isobutane[a]	assignment[f]
1	285.01[b]					$\pi^*(b_2)$, $^1B_2$
2	286.6		286.4			π^*(C═C, a_2), $^1B_2$
3		287.0		286.9	287.0	3s Ryd (^{t}Bu)
4	288.0	287.93(8)[c]	287.92(6)[d]	287.92[e]	287.8	$\pi^*(CH_3)$/3p (^{t}Bu)
5	289.6	289.6	289.6	289.6	288.6	4s Ryd (^{t}Bu)
6 br	293	292	293	292	292.4	σ^*(C−C)
7 br	302				301	σ^*(C−C), σ^*(C−H)

[a] Isobutane energies and term values from the published C 1s spectrum.[38] [b] Calibration relative to the C 1s → π^* transition of CO, ΔE = −2.32 eV. [c] Calibration relative to the N 1s → π^* transition of N_2, ΔE= −113.17(6) eV. [d] Calibration relative to the C 1s → π^* transition of CO_2, ΔE = −2.82(2) eV. [e] Calibration relative to the C 1s → π^* transition of CO_2, ΔE = −2.82 eV. [f] C_{2v} symmetry labels are used for convenience in the case of the C_2 symmetry molecules **2** and **4**.

Table 6. Energies (eV) and Assignments of Features in the N 1s Spectra of Silylenes (R_2Si:) and Dihydridosilanes (R_2SiH_2)

no.	1	2	3	4	assignment[e]
1	400.0[a]	399.6[b]			$\pi^*(b_2)$, $^1B_2$
2	402.0		401.2[c]		$\sigma^*(b_1)$ $^1A_1$,$^1B_1$; $\pi^*(a_2)$ $^1B_2$
3		401.8		401.3[d]	$\sigma^*(b_1)$, $^1A_1$,$^1B_1$
4 br		404	404	404	σ^*(N−C)
5 br	406	406	406	406	σ^*(N−C)

[a] Calibration relative to the C 1s → π^* transition of CO, ΔE = +109.25(6) eV. [b] Calibration relative to the N 1s → π^* transition of N_2, ΔE = −1.51(3) eV. [c] Calibration relative to the C 1s → π^* transition of CO_2, ΔE = +110.46(5) eV. [d] Calibration relative to the C 1s → π^* transition of **4,** ΔE = +113.4(1) eV. [e] C_{2v} symmetry labels are used for convenience in the case of the C_2 symmetry molecules **2** and **4**.

GSCF3 calculation of **I** (see Table 2), both transitions are expected in this energy range. In **2** and **4**, the π^*-(a_2) level is absent. Consistent with this, feature 3 in the spectra of **2** and **4**, which is assigned to N 1s → σ^*-(b_1) transitions, is much weaker than feature 2 in the spectra of **1** and **3**. The breadth and relative weakness of feature 3 in **2** and **4** is consistent with our assignment of feature 2 in **1** and **3** to the overlap of N 1s → $\sigma^*(b_1)$ and N 1s → $\pi^*(a_2)$ transitions.

Since nitrogen is coordinated by groups other than H in **1**−**4** (e.g., Si, the ring carbons, and the *tert*-butyl group), Rydberg transitions are very unlikely in the N 1s spectra. This is consistent with the N 1s spectra of substituted ureas and carbamates, in which the N 1s → Rydberg transitions observed at $-NH_2$ groups in urea and ethyl carbamate are strongly attenuated when the hydrogen atoms are replaced by bulky phenyl groups.[24] On the basis of a comparison to the N 1s spectra of species with C−N single bonds, the N 1s → $\sigma^*(b_1, N-C_{t-Bu})$ and N 1s → $\sigma^*(b_2, N-C_{t-Bu})$ transitions are expected to contribute in the 404−408 eV region.

3.5. Comparison to Spectral Simulations Based on ab Initio Calculations. Figure 6 presents the simulated Si 1s, N 1s, and C 1s spectra of **I** and **II**, derived from GSCF3 calculations (bottom traces), in comparison to the corresponding experimental spectra of **1** and **2** (upper traces). The GSCF3 calculations for the C 1s core excitation spectra of the model structures **I** and **II** are only for the ring carbon atoms and, thus, do not include the methyl contribution from the models **I** and **II**. To allow a valid comparison to the contribution of the two ring carbons, an appropriately scaled spectrum of isobutane[38] has been subtracted from the experimental spectra of **1** and **2** to remove the contributions of the t-Bu groups. Overall, there is excellent agreement between calculation and experiment, indicating the GSCF3 results provide a sound basis for spectral interpretation.

Figure 7 presents a schematic of the calculated term values for the first three core excitations and plots the molecular orbitals involved, as sampled with the core hole in the Si 1s level. The shapes of the MOs with the core hole located at the ring carbon or nitrogen atoms are very similar. However, the location of the core hole has an effect on the term value of the core excitation and level ordering, as shown graphically in Figure 7 and numerically in Table 2. Essentially, the $\pi^*(b_2, Si-N)$ level is strongly stabilized by placing the core hole on the Si, with less stabilization with the core hole on N and the least amount on C. Similarly, the $\pi^*(a_2, C=C)$ level is most stabilized with the core hole on the ring carbon atom, and the σ^* (b_1, Si−N) level is stabilized with the core hole on the Si or N atoms.

4. Discussion

The presence of a low-energy feature in each core excitation spectrum (Si ns, Si 2p, N 1s, C 1s) of the unsaturated silylene **1** illustrates that the lowest π^*-(b_2) orbital is delocalized over all of the atomic sites on the silylene ring. This is emphasized in Figure 8, which summarizes the experimental results for **1** and connects the calculated site density of the $\pi^*(b_2)$ LUMO and the

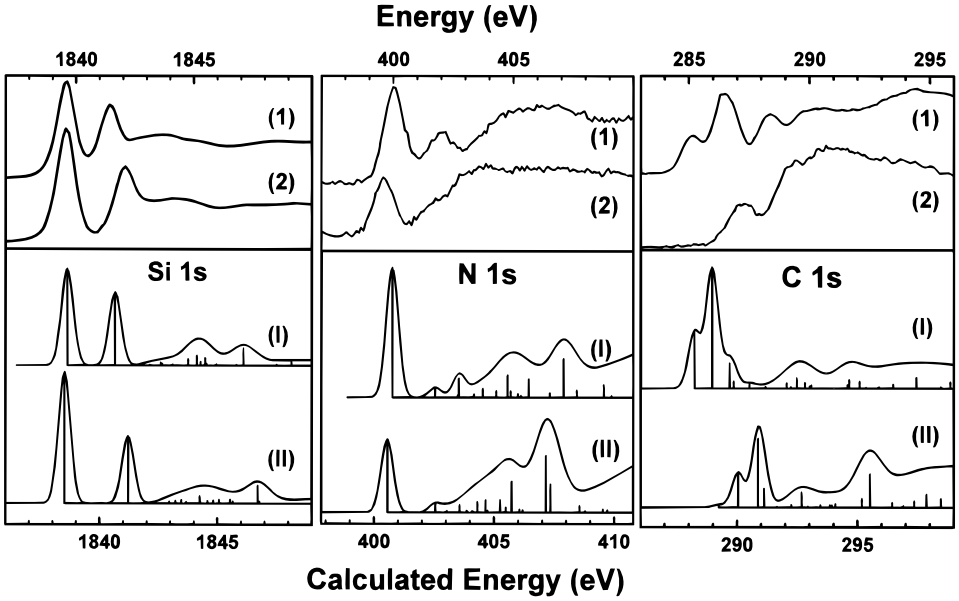

Figure 6. Comparison of the experimental Si 1s, C 1s, and N 1s core excitation spectra of silylene **1** and saturated silylene **2** to the Si 1s, C 1s, and N 1s core excitation spectra of the model silylene (**I**) and the model saturated silylene (**II**), calculated by improved virtual orbital (IVO) ab initio methods. The C 1s signals plotted are the difference of the measured spectra of **1** and **2** (see Figure 4) and that of isobutane,[38] scaled to remove the contribution from the two *tert*-butyl groups.

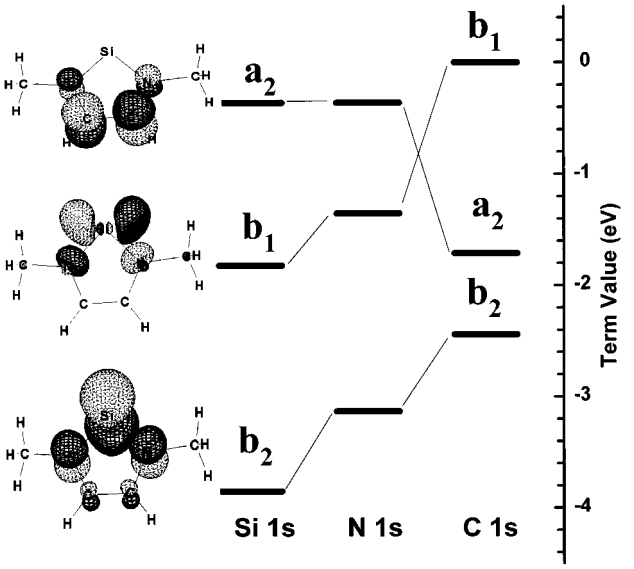

Figure 7. Calculated term values for excitation from the Si 1s, N 1s, and ring C 1s excitation in **I** to the three lowest energy levels: π^*(Si−N, b_2), σ^*(Si−N, b_1), π^*(C═C, a_2). The MO plots are from the calculation with a Si 1s core hole. The calculated MOs are very similar in shape when the core hole is placed on the N 1s or ring C 1s level.

relative intensities of the core → $\pi^*(b_2)$ transition in each core excitation spectrum. (A more complete comparison of the experimental results for **1** and the GSCF3 calculated spectra of **I** has been presented in Figure 6 and discussed in the preceding section.) The b_2 LUMO has a dominant Si 3p character, consistent with a simple Si $3s^23p^2$ configurational description of the divalent Si site. However there is also a considerable contribution from the other ring atoms, which is consistent with ($4n$ + 2) π delocalization as an important mechanism stabilizing **1**.[2] Removal of the C═C double bond in **2** strongly perturbs the electronic and geometric structure relative to **1**, generates a more isolated Si 3p character to the LUMO, and reduces the contribution from the N and especially C ring atoms to the $\pi^*(b_2)$ LUMO.

Clearly, divalent silylenes are characterized by an intense, low-energy Si 1s → π^* resonance associated with the strong Si 3p−π character of the LUMO. Additionally, the lowest Si 1s → σ^* transition varies strongly with the molecular structure of the heterocycle ring containing the silylene unit. The dramatic spectral variations through this series of molecules demonstrate the capabilities of core excitation spectroscopy as a probe for delocalization, especially in highly symmetric aromatic systems. Inorganic heterocycles, with their multitude of core levels of different symmetries, are a particularly fruitful area of application of this spectroscopy. Core excitation spectroscopic and computational studies are presently in progress on the isoelectronic divalent carbenes[39] and germylenes, along with their tetravalent analogues.

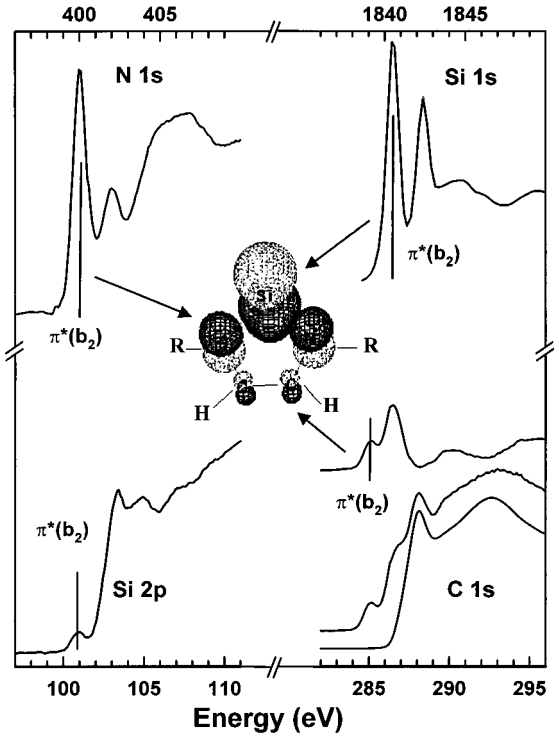

Figure 8. Summary of the experimental core spectra of **1** to emphasize the use of multilevel core excitation as a probe of ring delocalization. The MO plot is that calculated for the π^*(Si−N, b_2) MO in Si 1s excited **I**. Note that this plot also illustrates isolation of the ring carbon contribution to the total C 1s spectrum of **1** by subtraction of the spectrum of isobutane.[38]

Acknowledgment. This research was financially sponsored by NSERC (Canada). S.G.U. acknowledges the support of an Ontario Graduate Fellowship. This work is based in part on research conducted at the Synchrotron Radiation Centre, University of Wisconsin-Madison, which is supported by the NSF under award DMR-9212658. We thank Dr. X. H. Feng for his assistance with the operation of the CSRF DCM at SRC. Computing facilities (SPARTAN, IBM RS-6000) were provided by the Department of Chemistry (McMaster). We thank M. A. Brook for reviewing the manuscript and for helpful comments, M. Malott for assistance with SPARTAN calculations, and N. Kosugi for providing the GSCF3 code and advice on its operation.

OM9709188

(39) Denk, M. K.; Thadani, A.; Hatano, K.; Lough, A. *Angew. Chem. Int. Ed. Engl.* **1997**, *23*, 2607.
(40) Sodhi, R. N. S.; Brion, C. E. *J. Electron Spectrosc.* **1984**, *34*, 363.